

**RT SOLUTIONS, Inc.**

9 Channing Street, Cambridge, MA 02138.

# Final Report O3SAF-VS, 2007

## **Reflectance Templates for the O<sub>2</sub> A-band OCRA-ROCINN algorithm as applied to GOME-2 retrieval of cloud properties**

Robert J. D. Spurr<sup>(1)</sup>  
Diego Loyola<sup>(2)</sup>

<sup>(1)</sup>*Director, RT Solutions, Inc.  
9 Channing Street, Cambridge, MA 02138*

<sup>(2)</sup>*German Aerospace Center (DLR)  
Remote Sensing Technology Institute (IMF)  
PO Box 1116, D-82234 Wessling, Germany*

31 August 2007

*Contractual*  
Jukka Kujanpaa  
Finnish Meteorological Institute,  
P.O.BOX 503, FIN-00101 Helsinki, Finland

# Oxygen A Band Reflectance Templates for GOME-2 ROCINN

## 1. Introduction

This Final Report summarizes work done under a 2007 O3 SAF Visiting Scientist (VS) grant to upgrade the O<sub>2</sub> A-band reflectance templates as required for application of the ROCINN (Retrieval Of Cloud Information by Neural Networks) algorithm to the retrieval of cloud parameters from backscatter measurements from the GOME-2 spectrometer. The GOME-2 instrument (on board the METOP-1 Satellite) was launched successfully on October 19<sup>th</sup> 2006 from the Baikonur proving grounds. Like its predecessor GOME-1, GOME-2 has four linear array detectors; these four channels range from 240 to 800 nm with moderate resolution, and there are a number of polarization measurement devices.

Reflectance templates are tables of simulated sun-normalized satellite radiances calculated using a radiative transfer model. For GOME-1, radiances are calculated over the range 758 to 771 nm, which includes part of the continuum outside the oxygen A-band as well as the main features of the absorption band itself. Simulations are performed at high resolution before convolving to the GOME-1 resolution (about 60 points in the above range). Convolutions are performed using an analytic Gaussian function for the Channel 4 GOME-1 instrument response function. These tables are used as training data sets for the ROCINN algorithm; optimized sets of neural network weights and biases are then used in the ROCINN inverse model to deliver the requisite cloud information (cloud-top height and cloud-top albedo). The algorithm assumes the IPA holds for partially cloudy scenes, with the fractional cloudiness derived from a separate algorithm.

Separate tables were developed for reflectances from clear sky simulations (ground surface, assumed Lambertian) and fully cloudy scenarios (cloud-top surface, also assumed Lambertian). Reflectances are generated for a number of reflecting surface heights and albedos, and for a representative range of solar/satellite viewing conditions. Earlier versions of the ROCINN algorithm used templates based on straightforward transmittance calculations. A more recent version of the GOME-1 ROCINN algorithm employed the LIDORT radiative transfer code to deliver templates for a Rayleigh-scattering atmosphere.

The present report describes new template calculations done for GOME-2 application of ROCINN. There are two points of departure from previous work: (1) the use of the *vector* radiative transfer model VLIDORT for the simulation of *polarized* radiances in an aerosol-scattering atmosphere; and (2) the use of specific GOME-2 slit function information. The ROCINN algorithm is summarized in the next section. In Section 3 we outline the atmospheric optical model and some aspects of the VLIDORT radiative transfer simulations. Section 4 contains a summary of the reflectance tables.

## 2. The ROCINN algorithm

ROCINN [Loyola, 2004] is a new algorithm based on O<sub>2</sub> A band reflectances from optical remote sensing instruments: it delivers cloud-top height and cloud-top albedo. The independent pixel approximation is used; the cloud fraction  $c_f$  derived from a threshold algorithm (for GOME, this is the OCRA algorithm) is taken as a fixed input to the ROCINN algorithm. Surfaces are assumed Lambertian reflectors. The forward model reflectivity is then:

# Oxygen A Band Reflectance Templates for GOME-2 ROCINN

$$R_{sim}(\lambda) = c_f \langle R_c(\lambda, \Theta, c_a, c_z) \rangle + (1 - c_f) \langle R_s(\lambda, \Theta, s_a, s_z) \rangle \quad (1)$$

Here,  $\langle R \rangle$  denotes the convoluted reflectance to cloud-top or surface for path geometry  $\Theta$  (solar zenith angle and line-of-sight angle), wavelength  $\lambda$ , surface albedo  $s_a$  and cloud-top albedo  $c_a$ , and lower boundary heights  $s_z$  (surface) and  $c_z$  (cloud-top). For a scattering atmosphere, the reflectances are sun-normalized backscatter radiances calculated by the LIDORT or VLIDORT model. Reflectivities must first be calculated on a high-resolution wave number grid using line-by-line spectroscopic information for the O<sub>2</sub> A band, before convolution to instrument resolution with the response function. Quantities  $s_z$  and  $s_a$  are the surface height and albedo, taken from a suitable database and assumed known. ROCINN aims to retrieve cloud-top height  $c_z$  and the cloud-top albedo  $c_a$ . Calculations based on Eq. (1) are used to create a complete data set of simulated reflectances for all viewing geometries and geophysical scenarios, and for various combinations of cloud fraction, cloud-top height and cloud-top albedo.

In ROCINN, the forward model function is represented by the set  $S = \{(X_i, Y_i)\}$  for  $i = 1, \dots, s$ . Inputs  $X$  are the parameters  $\{c_f, \Theta, s_a, s_z, c_a, c_z\}$ . The outputs  $Y$  are the simulated radiances  $\{R_{sim}(\lambda)\}$ . To generate an inverse data set, we first add normal distributed Gaussian measurement noise  $\varepsilon$  to the simulated radiances:  $R = R_{sim} + \varepsilon$ . We may now generate the inverse data set  $S^* = \{(X_i^*, Y_i^*)\}$  for  $i = 1, \dots, t$ , where now the input set  $X^*$  comprises the parameters  $\{R_{sim}(\lambda), c_f, \Theta, s_a, s_z\}$  and the output is now  $Y^* = \{c_a, c_z\}$ , the unknown cloud-top albedo and cloud-top height. A neural network  $NN_{INV}$  is finally trained with the *inverse* data set  $S^*$ , giving the result:

$$\{c_a, c_z\} = NN_{INV}(R_{sim}(\lambda), c_f, \Theta, s_a, s_z). \quad (2)$$

For more details on the application of ROCINN and OCRA to GOME measurements, see [van Roozendaal *et al.*, 2006]. This paper also contains a discussion on validation of the algorithm.

## 3. Radiative Transfer Modeling

### 3.1 VLIDORT Model and Updates

Earlier ROCINN templates for GOME-1 were based on scalar calculations using the LIDORT mode [Spurr, 2002]. It has been known for some time that the neglect of polarization in radiative transfer simulations of A-band radiances can be significant [Stam *et al.*, 1999]. We have used the VLIDORT radiative transfer model to calculate new templates for this ROCINN application to GOME-2. The VLIDORT model was developed as part of two previous VS activities for the Ozone SAF (2004 and 2005), and has been written up and published [Spurr, 2006].

VLIDORT is a multilayer multiple scattering vector discrete ordinate radiative transfer model for the simulation of polarized light radiation. It has a pseudo-spherical capability to deal with solar and line-of-sight beam attenuation in a curved atmosphere. The model is also fully linearized: it has the ability to generate analytic weighting functions of the Stokes field with respect to any atmospheric or surface parameter. VLIDORT has a full BRDF treatment for reflecting surfaces.

# Oxygen A Band Reflectance Templates for GOME-2 ROCINN

The model has been validated against a number of benchmarks in the literature. At the time of writing, VLIDORT appears in Version 2.2, and it has all the capabilities of its scalar counterpart LIDORT Version 3.3 (with the exception of thermal emission code). Both codes have been streamlined and reorganized so that inputs and outputs are consistent.

VLIDORT contains a new implementation of the exact computation of single scattering (and its linearization) in a curved atmosphere [Spurr, 2007]. This makes a precise calculation of the single scattering radiation field along the line-of-sight, allowing for spherical curvature of all incident solar beams as well as the line-of-sight itself. The original 'nadir-only' single scatter correction has been retained as an alternative to this new correction (the nadir-only correction does not allow for variation of the viewing angle with height, and thus the solar angle is the same all the way up the atmosphere). The old VLIDORT-PLUS models used a kind of 'super-environment' for outgoing-beam single scatter correction. The new Version 2.2 outgoing correction is extremely simple to use, being controlled by a single flag. It should be noted that the existing 'nadir-only' and the superseded VLIDORT-PLUS corrections were based on the approximate 'average-secant' parameterization of solar beam attenuation through any layer. The new outgoing correction dispenses with this approximation and is thus more accurate. The exact single-scatter correction is fully linearized with respect to all profile quantities (and for LIDORT, the total columns as well).

In the new version of VLIDORT, all input solar and viewing angles must be specified for viewing conditions at sea level (bottom of the atmosphere). This distinction is important for the outgoing line-of-sight sphericity correction. For reflecting surfaces which are at higher levels in the atmosphere, above the 'true' ground or BOA level at which the input geometries are specified, the 'true' BOA input geometries must be adjusted slightly (using trigonometry). A suitable adjustment routine has been incorporated. The exact single scattering calculation uses all the adjusted angles, whereas the diffuse-field calculation uses the original values of the solar zenith angles, but the adjusted values of the viewing angles.

Another improvement has been in the speed of VLIDORT. The code was given a partial optimization in March 2007, resulting in a much more compact usage of RAM and a speed enhancement of around 25-30% for an 11-layer 8-stream discretization. The code has also been partitioned, with the BRDF calculations now controlled by separate master modules. The present application does not require non-Lambertian surfaces, so the BRDF supplement is excluded in the compilation (along with the Jacobian or linearization packages). The LAPACK directory has also been upgraded to include latest numerical software codes.

## 3.2 Atmospheric Model

For each atmospheric layer, we have Rayleigh scattering optical depth  $\sigma_{Ray}$ , molecular absorption optical depth  $\alpha_{gas}$ , aerosol extinction and scattering optical depths  $\Delta_{Aer}$  and  $\sigma_{Aer}$  respectively. Then the *total optical property inputs* are given by:

$$\Delta = \alpha_{gas} + \sigma_{Ray} + \Delta_{aer}; \quad \omega = \frac{\sigma_{aer} + \sigma_{Ray}}{\Delta}; \quad \beta_l = \frac{\beta_{Ray,l}\sigma_{Ray} + \beta_{aer,l}\sigma_{aer}}{\sigma_{Ray} + \sigma_{aer}}. \quad (3)$$

# Oxygen A Band Reflectance Templates for GOME-2 ROCINN

Here,  $\Delta$  is the total layer optical thickness,  $\omega$  is the total layer single scattering albedo, and  $\beta_l$  are the total phase function Legendre expansion coefficients; these three quantities are the basic IOP (inherent optical property) inputs to the scalar LIDORT model. For the vector VLIDORT model, the phase function coefficients are replaced by 4 x 4 matrices of expansion coefficients.

An 11-layer atmosphere is used in the modeling, with resolution 1.0 km up to 4 km, 2.0 km from 4.0 to 12.0 km, and a coarser spacing up to the top-of-atmosphere level at 50 km. Top of atmosphere (TAO) is 60 km. Temperature and pressure profiles are taken from the USA Standard atmosphere, and interpolated to this grid. For trace gas absorption, we consider O<sub>2</sub> absorption over the GOME-2 spectral range 758 to 771 nm. Line-by-line O<sub>2</sub> absorption cross-sections are computed using an LBL model developed by R. Spurr, with line spectroscopic data from the HITRAN 2004 data base [Rothman *et al.*, 2005]. A resolution of 0.025 wave numbers was used for the basic calculations, resulting in some 10,560 points for each template to cover the desired GOME-2 range.

Rayleigh cross-sections and depolarization ratios are taken from a recent reappraisal [Bodhaine *et al.*, 1999]. For the aerosols, we use a LOWTRAN-aerosol specification of optical thickness values for a rural type of surface aerosol [Shettle and Fenn, 1979]. For the aerosol scattering properties, a Mie code [de Rooij and van der Stap, 1984] was used to generate suitable Mueller matrices of phase matrix expansions as required for the VLIDORT polarization calculations. Separate Mie calculations were done for the boundary layer (0-2 km), free troposphere (2-12 km) and stratospheric regimes (12-50km).

## 3.3 Convolution and table classes

For surface templates, we choose 5 albedos (0.02, 0.1, 0.3, 0.5 and 0.98) and 6 lower boundary heights (0.0, 0.5, 1.0, 2.0, 3.0, 4.0 km). For cloud-top reflectances, we choose 8 albedos (0.3, 0.4, 0.5, 0.6, 0.7, 0.8, 0.9 and 1.0) and 16 lower boundary heights (0.0, 0.5, 1.0, 2.0 and at 1 km intervals to 14.0 km). 10 solar zenith angles ranging from 15° to 88° were used, along with 5 values of the relative azimuth angle between the solar and scattering planes (0°, 45°, 90°, 135° and 180°), and (new for GOME-2), a set of 11 viewing zenith angles from 0° to 50° at intervals of 5°. All VLIDORT simulations were done using the pseudo-spherical approximation, with exact calculations of the single scatter component in all cases. In all cases, 8 discrete ordinate streams were used for the multiple scatter quadratures.

Template radiances are specified at 62 GOME-2 wavelengths for Channel 4 between 758 and 771 nm, these wavelengths being part of the data set of slit functions computed at RAL and provided for this study by S. Slijkhuis (private communication). Note that the slit function shape is specified uniquely by 141 points at each wavelength, although parameters for fitted functions (Gaussians) are provided as ancillary data. Slit function amplitudes are given at 141 points within  $\pm 0.7$  nm of an assigned wavelength for channels 1 and 2 and within  $\pm 1.4$  nm of an assigned wavelength in Channels 3 and 4. High-resolution calculations at 0.025 wave numbers were convolved to the GOME-2 wavelengths using this slit function data.

# Oxygen A Band Reflectance Templates for GOME-2 ROCINN

## 4. The templates

Figure 1 is an illustration of a typical template calculation, in this case for the highest cloud boundary (14 km) and albedo 0.3. Results are plotted for eight solar zenith angles from  $15^\circ$  to  $85^\circ$ , for a direct nadir satellite view, and for an azimuth of  $0^\circ$ . (Nadir viewing is not azimuth-independent in polarized radiative transfer). In the upper panel, the high-resolution calculation is shown beneath the convolved results. With the table classification as noted above, there are 30 surface templates and 128 cloud-top templates, each template data set comprising 550 lines of output corresponding to the 550 solar/satellite viewing geometry combinations. Each line contains the height and albedo, the trio of geometrical angles, the wavelength and 62 reflectivity values for these wavelengths. There is also an indication of the aerosol type (0 = Rayleigh-only, 1 = land surface boundary layer aerosol, 2 = sea surface boundary layer aerosol) and the season (0 = Rayleigh only, for aerosols: 1 = winter, 2 = summer).

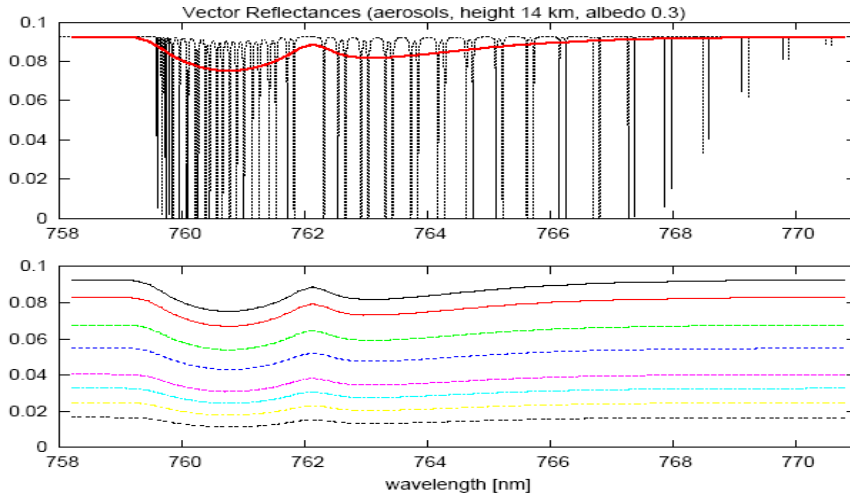


**Figure 1.** GOME-2 ROCINN templates example (see text for details).

Polarized radiative transfer is computationally expensive. A full 11-layer vector-mode calculation (with aerosols) for 10,560 wave-numbers takes several hours on the RT Solutions Dell 8400 3.8 GhZ computer, so the work has been farmed out to a cluster of computers at DLR.

The computer environment for generating these tables has a number of options. VLIDORT can be run in scalar mode (no polarization); furthermore, there is an option for Rayleigh-only calculations (no aerosols). In all, some 8 Zipped tarballs have been created; these are called 'GRS.gz', 'GRV.gz', 'CRS.gz', 'CRV.gz', 'GAS.gz', 'GAV.gz', 'CAS.gz', 'CAV.gz', where G = ground, C = Cloud-top, R = Rayleigh-only, A = Aerosol included, S = Scalar, V = Vector (with polarization).

# Oxygen A Band Reflectance Templates for GOME-2 ROCINN

## Acknowledgments

The authors would like to thank Vijay Natraj (Caltech/JPL) for provision of aerosol data from the Meerhoff Mie program.

## 5. References

- Bodhaine, B., N. Wood, E. Dutton, and J. Slusser, On Rayleigh optical depth calculations, *J. Atmos. Ocean. Tech.*, **16**, 1854-1861, 1999.
- Loyola, D., Automatic Cloud Analysis from Polar-Orbiting Satellites using Neural Network and Data Fusion Techniques, *IEEE International Geoscience and Remote Sensing Symposium*, **4**, 2530-2534, Alaska (2004)
- de Rooij, W.A., and C.C.A.H. van der Stap, Expansion of Mie scattering matrices in generalized spherical functions, *Astron. Astrophys.*, **131**, 237-248 (1984).
- Rothman, L., et al., The HITRAN 2004 Molecular Spectral Database, *Journal of Quantitative Spectroscopy and Radiative Transfer*, vol. **96**, 139-204 (2005).
- Shettle E. P., and R. W. Fenn, Models for the aerosols of the lower atmosphere and the effects of humidity variations on their optical properties, Air Force Geophysics Laboratory, Hanscomb Air Force Base, Mass. (1979).
- Spurr, R., Simultaneous derivation of intensities and weighting functions in a general pseudo-spherical discrete ordinate radiative transfer treatment. *J. Quant. Spectrosc. Radiat. Transfer*, **75**, 129-175 (2002).
- Spurr, R., VLIDORT: A linearized pseudo-spherical vector discrete ordinate radiative transfer code for forward model and retrieval studies in multilayer multiple scattering media, *J. Quant. Spectrosc. Radiat. Transfer*, 102(2), 316-342, doi:10.1016/j.jqsrt.2006.05.005 (2006).
- Spurr, R., LIDORT and VLIDORT: Linearized pseudo-spherical scalar and vector discrete ordinate radiative transfer models for use in remote sensing retrieval problems, *Light Scattering Reviews*, VOLUME 3, in press, ed A. Kokhanvsky, Springer (2007).
- Stam, D.M., J.F. de Haan, J.W. Hovenier, P. Stammes, Degree of linear polarization of light emerging from the cloudless atmosphere in the oxygen A band. *J. Geophys. Res.*, **104**, 16843 (1999).
- Van Roozendael, M., D. Loyola, R. Spurr, D. Balis, J-C. Lambert, Y. Livschitz, P. Valks, T. Ruppert, P. Kenter, C. Fayt, and C. Zehner, Ten years of GOME/ERS2 total ozone data: the new GOME Data Processor (GDP) Version 4: I. Algorithm Description, *J. Geophys Res.*, doi: 10.1029/2005JD006375 (2006).